

High dielectric constant and frozen macroscopic polarization in dense nanocrystalline BaTiO₃ ceramics

Maria Teresa Buscaglia,¹ Massimo Viviani,¹ Vincenzo Buscaglia,^{1,*} Liliana Mitoseriu,^{2,3} Andrea Testino,^{1,3} Paolo Nanni,^{1,3} Zhe Zhao,^{4,†} Mats Nygren,⁴ Catalin Harnagea,⁵ Daniele Piazza,⁶ and Carmen Galassi⁶

¹*Institute for Energetics and Interphases, Department of Genoa, National Research Council, Via de Marini 6, I-16149 Genoa, Italy*

²*Department of Solid State and Theoretical Physics, Al. I. Cuza University, Bv. Carol I 11, 700506 Iasi, Romania*

³*Department of Chemical and Process Engineering, University of Genoa, Piazzale Kennedy, I-16129 Genoa, Italy*

⁴*Department of Inorganic Chemistry, University of Stockholm, S-106 91 Stockholm, Sweden*

⁵*INRS-Energie, Matériaux et Télécommunications, University of Québec, 1650 Lionel-Boulet, Varennes, Québec, Canada J3X 1S2*

⁶*Institute of Science and Technology for Ceramics, Via Granarolo 64, I-48018 Faenza, Italy*

(Received 6 October 2005; revised manuscript received 2 December 2005; published 24 February 2006)

Theoretical models for small ferroelectric particles predict a progressive decrease of the Curie temperature, spontaneous lattice strain, and polarization until the critical size corresponding to transition to the cubic phase and disappearance of ferroelectricity is reached. In contrast, the behavior of nanocrystalline BaTiO₃ ceramics with a grain size of ≈ 30 nm is dominated by extrinsic effects related to the grain boundaries which mask the expected downscaling of properties. While the noncubic crystal structure, the high dielectric constant (≈ 1600) and the variation of permittivity with temperature suggest a ferroelectric behavior, very slim, and nearly linear polarization hysteresis loops are observed. Evidence for the existence of a ferroelectric domain structure with domains extending over several grains and of polarization switching at local scale is given by piezoresponse force microscopy. The suppression of macroscopic ferroelectric hysteresis and switching originates from a frozen domain structure stable under an external field owing to the effects exerted by the grain boundaries, such as the clamping of the domain walls and the hindrance of polarization switching. Furthermore, the depolarization field originated by the low-permittivity nonferroelectric grain boundaries can cause a significant reduction of polarization. If the grain size is small enough, the ceramic is expected to undergo a “phase transition” to a polar phase with nonswitchable polarization. The BaTiO₃ ceramics with grain size of 30 nm investigated in the present study are deemed to be close to this transition.

DOI: [10.1103/PhysRevB.73.064114](https://doi.org/10.1103/PhysRevB.73.064114)

PACS number(s): 77.84.-s, 81.07.-b, 68.37.-d

I. INTRODUCTION

Among the ferroelectric materials, polycrystalline barium titanate (BaTiO₃, BT) finds extensive application (yearly production: ≈ 11 000 tons) in the electronic industry as dielectric in ceramic capacitors and, particularly in multilayer ceramic capacitors (MLCCs) because of its high relative dielectric constant (1500 to 5000 depending on grain size) and low losses.¹ The continuous advance in microelectronics and communications is gradually leading to the miniaturization of ferroelectric components and of MLCCs. To be able to achieve high capacitance in a small volume, the dielectric layer thickness has to be reduced while increasing the total number of layers. The dielectric thickness will become $< 1 \mu\text{m}$ in a very near future and the number of layers could exceeds 1000.² The permittivity (ϵ_r) of BT ceramics increases with decreasing grain size, passing through a maximum ($\epsilon_r \approx 5000$) around $0.8-1 \mu\text{m}$.^{3,4} On further decreasing the grain size, a rapid decrease of ϵ_r is observed. This drop can pose important limitations to the miniaturization of MLCCs. If the dielectric layer has to be comprised of at least 5–7 grains for reasons of mechanical strength and to achieve a uniform thickness, it is clear that the grain size in layers of the order of $0.7 \mu\text{m}$ or less will be ≤ 100 nm. Consequently, it is of large practical interest to prepare dense nanocrystalline BaTiO₃ ceramics and to investigate their dielectric characteristics. This should provide important indications for the design of next generations MLCCs.

From a fundamental point of view, there is a general agreement that the reduction of the physical sizes of ferroelectrics such as BaTiO₃ and PbTiO₃ leads to a progressive decrease of the spontaneous polarization. Models based on the Landau-Ginzburg-Devonshire theory of ferroelectrics where surface and gradient effects are taken into account predict a critical size from a few nm to a few tens of nm (Ref. 5) for disappearance of ferroelectricity (suppression of spontaneous polarization) in isolated particles. The surface effect is also responsible for other phenomena, such as the smearing of the phase transition observed in ferroelectric thin films.⁶ Experimental studies give some support to the existence of such a critical size, even though there is a very broad dispersion in the data owing to the influence of several extrinsic effects which change with the size of the system.^{7,8} In general, the mechanical and electrical boundary conditions as well as the presence of defects can have a strong influence on the ferroelectric and dielectric properties when the dimensions of the system are reduced below 100 nm .^{7,9,10} New results obtained on thin films and first-principles atomistic calculations suggest that ferroelectric behavior should still persist down to a size of few nm.¹¹ Accordingly, Saad *et al.*¹² reported no variation of dielectric and phase transition behavior in free-standing thin BaTiO₃ single crystals down to a thickness of 75 nm. In ceramics, the surface effects are less important, while the internal stresses originated during the cooling through the Curie temperature¹³ and the

grain boundaries play a major role in determining a change of the properties with decreasing grain size. In the case of BT ceramics, the critical size has been estimated to be in the range 10–30 nm.¹⁴ Concerning the dielectric properties, recent studies^{14–17} have shown that the “dilution effect” related to the presence of a lower permittivity nonferroelectric grain boundary (dead) layer can considerably contribute to the drop of permittivity in submicron and nanocrystalline BT ceramics and thin films. Such a dead layer not necessarily corresponds to the presence of a secondary phase, but could be accounted for by a shell of BT with disordered/defective structure or nonswitchable polarization close to the surface of the grains. The estimated thickness of the dead layer is comparable to the correlation length in ferroelectric perovskites (1–3 nm), i.e., the scale on which the polarization changes near the surface.

In this study we report the dielectric and ferroelectric properties of dense nanocrystalline BaTiO₃ ceramics with a grain size of 30 nm. No previous results are available in the literature for dense materials with such a small grain size. Even a moderate porosity level can strongly depress the permittivity of the ceramic¹⁸ and, as a result, porous materials have a marginal interest. The very recent study of Guo *et al.*¹⁹ concerns the electrical conductivity of a ceramic with similar grain size, but ferroelectric properties were not reported.

II. EXPERIMENTAL

Ultrafine particles of BT were prepared by solution precipitation as described in detail elsewhere.²⁰ The synthesis conditions were selected in order to have a small TiO₂ excess. It is well known that the presence of a small TiO₂ excess in barium titanate inhibits grain growth below the temperature (≈ 1250 °C) corresponding to the onset of abnormal grain growth and this is advantageous for obtaining fine-grained ceramics.²¹ The Ba/Ti ratio of the powder was estimated to be ≈ 0.995 by inductively coupled plasma spectroscopy. The main impurity contained in the powders was Na (≈ 600 ppm), while Sr was < 50 ppm. The specific surface area of the powder was measured by nitrogen adsorption according to the BET method and was ≈ 75 m² g⁻¹. The equivalent particle diameter was 16 nm, in agreement with the crystallite size (13 nm) determined from x-ray diffraction (XRD). Observation by transmission electron microscopy has shown well defined single-crystal particles of 10–20 nm.

The powder was densified for 3 min at 1000 °C in the form of disks (1.2 cm diameter, 0.1–0.2 cm thickness) by means of spark plasma sintering (SPS) using the same setup described in a previous paper.¹⁴ After sintering, the ceramics were polished and then annealed in air for 2 h at 700 °C. This treatment was intended to relieve the residual stresses (arising either from the SPS process or from polishing) and remove the surface carbon contamination. The graphite die used as sample holder can induce reducing sintering conditions with oxygen loss from the lattice and formation of oxygen vacancies in the ceramic. Therefore a further result of the post-annealing treatment is the removal of the excess oxygen vacancies possibly produced during SPS treatment.

Microstructure was characterized by scanning electron microscopy (SEM) (LEO 1450VP, LEO Electron Microscopy, Ltd., Cambridge, UK) and atomic force microscopy (AFM) (DI-Enviroscope, Veeco Instruments, Santa Barbara, CA) equipped with SuperSharp Silicon tips from Nanosensors (Neuchatel, Switzerland). Phase composition and crystal structure were investigated by x-ray diffraction (XRD) (Co K α radiation, Philips PW1710, Philips, Eindhoven, The Netherlands). Sputtered gold electrodes were applied on the upper and lower surfaces of the polished and post-annealed sintered disk obtaining a parallel-plate capacitor configuration. Permittivity, resistivity and impedance measurements were performed at 10²–10⁵ Hz using an impedance analyzer (Solartron SI1260) in the temperature range 40–180 °C (heating/cooling rate of 0.5 °C/min) with an applied voltage of 1 V. Macroscopic-polarization-electric-field $P(E)$ hysteresis measurements were performed at room temperature using a modified Sawyer-Tower circuit for different field amplitudes from 10–80 kV cm⁻¹ at a frequency of 50 Hz. Local switching properties were investigated by piezoresponse force microscopy. A computer-controlled lock-in amplifier (Signal Recovery, Model 7265) was connected to the AFM via a signal access module. To apply the voltage to the sample, conductive cantilevers CSC11A (spring constant 0.6 N/m) coated with semiconductor W₂C from Micromash (Portland, USA) were used. An ac testing voltage (32 kHz, 0.5 V for imaging and 0.25 V for local hysteresis) was applied between the tip and the bottom electrode of the ceramic sample. Hysteresis measurements were obtained by superimposing the output of a voltage amplifier (model SA10 from Sensor Technology, Collingwood, ON) over the ac testing voltage. The input of the amplifier was fed to an auxiliary digital to analog converter of the lock-in amplifier, computer-controlled using custom software developed under the Testpoint platform.

III. RESULTS AND DISCUSSION

Microstructure. The relative density of the samples, determined by Archimedes’ method, resulted in $\approx 97\%$ of the theoretical density (6.02 g cm⁻³). Observation on fracture surfaces by SEM and of polished surfaces of post-annealed samples by AFM revealed an homogeneous microstructure with average grain size of ≈ 30 nm, as shown in Fig. 1. The AFM tips having a tip radius at the apex below 5 nm (according to the manufacturer, typically 2 nm), enabled the detection of grains having 3 nm in lateral size, on a surface with a roughness of 2 nm over 1 μ m \times 1 μ m area. More than 90% of the grains have sizes between 10 and 50 nm, as can be appreciated from Fig. 1(c). Similar distributions were obtained in other locations of the sample. The XRD patterns of the ceramics (Fig. 2) do not show the characteristic splitting of tetragonal BaTiO₃ and correspond, at a first glance, to the Pm3m cubic symmetry. However, an indication about the existence of a lower crystal symmetry is provided by the fact that the peaks corresponding to the 111 and 222 reflections, which are not subjected to splitting during the cubic to tetragonal transformation, are narrower than the other peaks. Therefore, the observed pseudocubic XRD patterns are the

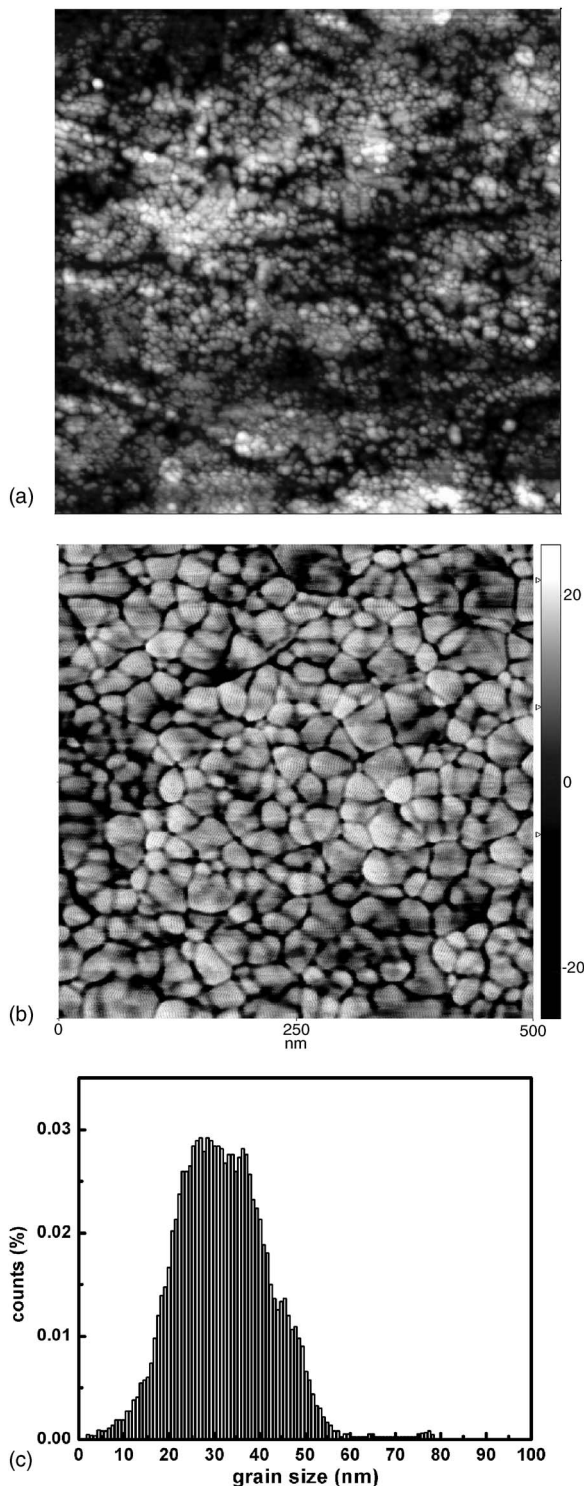


FIG. 1. AFM topography of the surface of a dense nanocrystalline BaTiO₃ ceramic with mean grain size of ≈30 nm. (a) Scan image, low magnification (scan area 2000×2000 nm²). The scratches on the surface come from polishing. (b) Phase image, high magnification (scan area 500×500 nm²). (c) Grain size distribution.

result of a small spontaneous lattice strain and the broadening effect related to the small grain size. The crystallite size determined from the broadening of the 111 and 222 peaks using Scherrer equation was 34 nm. Secondary phases, if

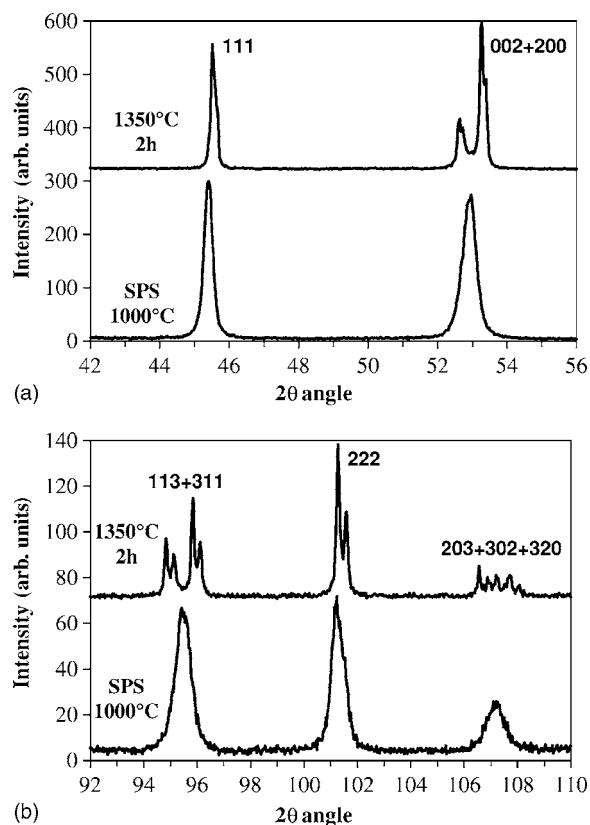


FIG. 2. Comparison of the x-ray diffraction patterns of a BaTiO₃ ceramic with grain size of ≈30 nm obtained by spark plasma sintering (lower trace) and of a coarse ceramic prepared by conventional sintering at 1350 °C (upper trace) from the same powder. (a) Region around the 111 reflection. (b) Region around the 222 reflection.

any, are below the XRD detection limit. The tetragonal deformation of the lattice, defined as $100(c/a-1)$ (c and a are the tetragonal lattice parameters) was evaluated by the Rietveld refinement method to be ≈0.25, i.e., only $\frac{1}{4}$ of the value (1) reported for coarse ceramics and single crystals.²² The tetragonal structure ($c/a=1.01$) is fully restored after sintering the powder at 1350 °C (Fig. 2). According to the phase diagram of Rase and Roy²³ and to electrical conductivity measurements²⁴ as well as to high-temperature annealing experiments we have carried out on BT powders containing different amounts of excess titania, the solubility of TiO₂ in the perovskite lattice is roughly estimated to be ≈1 at. %. Consequently, excess titania contained in the present samples is likely to be accommodated in the homogeneity range of BaTiO₃ with creation of barium and oxygen vacancies rather than forming second phase particles. However, the segregation of a very thin layer of a Ti-rich phase at the grain boundaries can not be excluded.

Dielectric properties. The relative dielectric constant ϵ_r of nanocrystalline BT [Fig. 3(a)] is remarkably high (1500–1650 at 70 °C) considering the very small grain size of the ceramic. The dielectric loss $\tan \delta$ is rather low, less than 5% for the whole temperature and frequency range investigated [Fig. 3(b)]. Measurements carried out at room temperature showed that $\tan \delta$ is of the order of 2% in the range

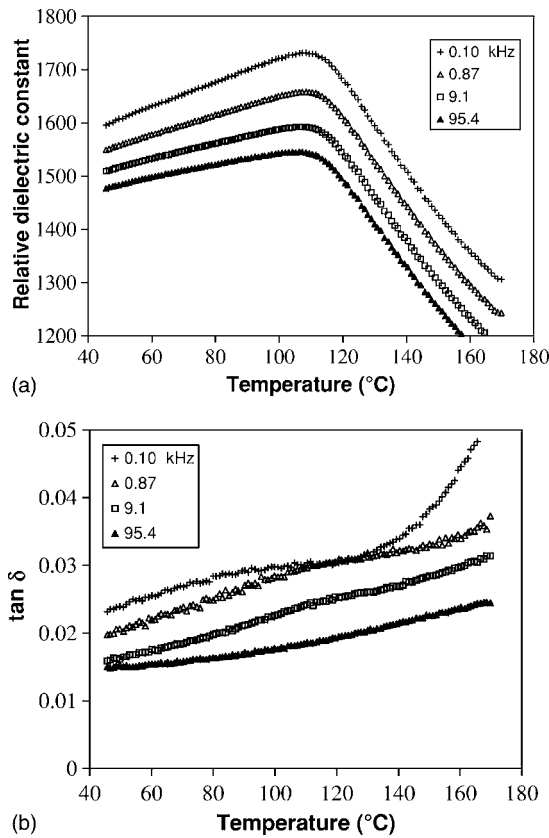


FIG. 3. Dielectric properties of a dense nanocrystalline BaTiO₃ ceramic with grain size of ≈30 nm at different frequencies. (a) Relative dielectric constant. (b) Loss tangent tan δ.

0.1–10⁵ Hz. The dc resistivity is ≈10¹³ Ω cm at room temperature. The high temperature (350–750 °C) conductivity data showed an activation energy of 0.96 eV, in accordance with the value of 0.99 eV recently reported for nanocrystalline BaTiO₃ ceramics fabricated by hot pressing.¹⁹ In agreement with the general behavior reported in the literature, the decrease of grain size leads to the broadening and flattening of the permittivity anomaly located at the ferroelectric-to-paraelectric transition temperature (T_C). Thus the sharp peak of ϵ_r , centered at T_C typical of coarse ceramics is replaced by a rounded maximum, suggesting a more diffuse character of the phase transition. As a result, the variation of ϵ_r with temperature is strongly reduced, with a variation within ±5% in the range 40–130 °C. The maximum of the dielectric constant is located at 106 °C. For comparison, T_C in coarse grained ceramics (>10 μm) is 125–130 °C.²² The lowering of T_C with decreasing grain size reported in previous studies^{14,17} is thus confirmed, even though the shift seems less pronounced in the present case. The permittivity data in the paraelectric region ($T > T_C$) are well described by the Curie-Weiss law above 125 °C, with a Curie constant of ≈2 × 10⁵ K. The Curie-Weiss temperature θ turns out to be ≈–30 °C, to be compared to the reference value of ≈110 °C reported for single crystals and coarse grained ceramics,²² i.e., a lowering of ≈140 °C. As shown by Frey *et al.*¹⁵ and, more rigorously, by Emelyanov *et al.*,¹⁶ the lowering of θ with decreasing grain size is only apparent and

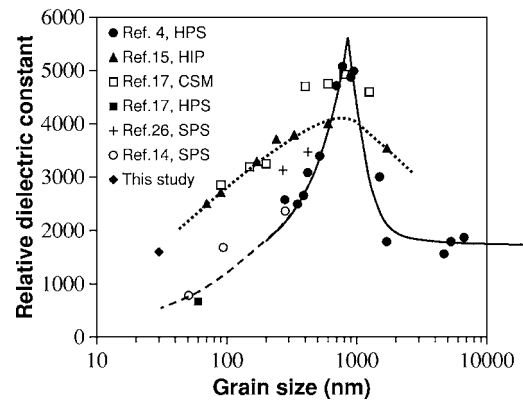


FIG. 4. Relative dielectric constant of BaTiO₃ dense ceramics obtained by different methods versus grain size at 70 °C. HPS: hot-pressing sintering, HIP: pseudoisostatic pressing in a multianvil press, CSM: combined sintering method, SPS: spark plasma sintering.

related to the presence of a grain boundary dead layer. A shift of the Curie-Weiss temperature was also observed in the case of polycrystalline Ba_(1-x)Sr_xTiO₃ thin films and ascribed to an “interface” effect.²⁵ The effective permittivity of fine polycrystalline BaTiO₃, considered as composed of ferroelectric grains with high permittivity separated by a continuous network of nonferroelectric grain boundaries with lower permittivity, still follows the Curie-Weiss law above T_C provided that the Curie constant and the Curie-Weiss temperature are properly renormalized as a function of grain size.^{14–16} The thickness d of the grain boundary dead layer is estimated using the analytical expression proposed by Emelyanov *et al.*¹⁶ as

$$\theta = \theta_0 - \frac{C_0 [g^3 - (g - 2d)^3]}{\epsilon_d [2g^3 + (g - 2d)^3]}, \quad (1)$$

where g is the grain size, C_0 and θ_0 are the Curie constant and the Curie-Weiss temperature of the ferroelectric region, respectively, and ϵ_d the relative dielectric constant of the grain boundary layer. The reference Curie-Weiss parameters of BaTiO₃ were taken to be $\theta_0 = 110$ °C and $C_0 = 1.8 \times 10^5$ K.^{15,16} The experimental value of $\theta = -30$ °C can be reproduced by setting $\epsilon_d \approx 100$ and $d \approx 1$ nm. The value adopted for ϵ_d was selected by considering that a relative dielectric constant of the order of 100 is typical of nonferroelectric perovskites and TiO₂ at room temperature. However, the measured value of θ can be also reproduced by setting $\epsilon_d \approx 50$ and $d \approx 0.5$ nm or $\epsilon_d \approx 200$ and $d \approx 2$, which are still physically sound combinations. A dead layer thickness of ≈1 nm seems typical of high-quality dense ceramics.^{15–17} In agreement, the relative dielectric constant of ≈1600 displayed at 70 °C by the 30 nm ceramics compares well with a value of ≈1700 that can be extrapolated from the permittivity data reported by Frey *et al.*¹⁵ and Polotai *et al.*¹⁷ (Fig. 4).

Irrespective of temperature, an almost constant difference of ≈150 in the values of ϵ_r measured at 0.1 and 100 kHz (Fig. 3) is found. This behavior is generally not observed in coarse BaTiO₃ ceramics, where the frequency dispersion in the paraelectric regime is usually lower than in the ferroelec-

tric phase. Even in systems showing a diffuse phase transition such as BaTiO₃ solid solutions or in relaxors, the dispersion, if present, is observed at temperatures lower than that corresponding to the maximum of the dielectric constant. Since the ceramics are insulating, the dispersion can not be related to residual electronic conduction. The peculiar response of the nanocrystalline ceramic is probably related to the different dielectric properties of the core of the grains and of the grain boundary region. This can lead to charge accumulation at the grain boundaries and Maxwell-Wagner polarization mechanism. The increase of the loss tangent at 100 Hz observed at temperatures above 140 °C (Fig. 3) may be an indication of such space charge effects.

The previous dielectric data show that properly processed, high-quality nanocrystalline BaTiO₃ ceramics can retain a high dielectric constant down to a grain size of a few tens of nm. It is clear that to meet this goal the thickness of the grain boundary dead layer has to be ≤ 1 nm. The sensitivity of the dead layer thickness to the processing conditions and to the nature of the starting powders can explain the broad dispersion of permittivity data for BaTiO₃ ceramics with grain size below 500 nm,^{4,14–17,26} as shown in Fig. 4. According to the available, albeit limited experimental data, it appears that the thickness of the dead layer is strongly dependent on the densification technique adopted for sintering¹⁷ as well as on the stoichiometry (Ba/Ti ratio) of the ceramic. In a recent and detailed study, Rühle and co-workers²⁷ have investigated the grain boundary structure of BaTiO₃ ceramics sintered at a relatively low temperature (1250 °C) and containing a small TiO₂ excess by means of high-resolution transmission electron microscopy (HRTEM) and electron energy loss spectroscopy (EELS). The results reveal the existence of a well-defined grain boundary structure. Many grain boundaries are faceted with small steps and long segments parallel to the {111} planes. These features are related to the presence of an ordered and very thin (thickness ≤ 0.8 nm) grain boundary layer. The EELS spectra show that the Ba/Ti ratio and the atomic bonding at the grain boundaries are different from those typical of the grain cores. Faceted grain boundaries were also observed by Lee *et al.*²⁸ These observations provide a strong indication about the physical nature of the dead layer, at least in Ti-rich barium titanate. The addition of a small TiO₂ excess might be an effective method to control the grain boundary structure and the thickness of the dead layer. Although a careful HRTEM investigation on stoichiometric and Ba-rich BaTiO₃ ceramics has not been performed yet, it is quite clear that in that case the grain boundary structure is completely different, with formation of more disordered and atomically rough grain boundaries.^{21,27} A further effect of a TiO₂ excess can be the modification of impurity segregation at grain boundaries. Acceptor species, such as Na⁺ (the main impurity of our powders), have a strong tendency to segregate at grain boundaries of BaTiO₃ and SrTiO₃ ceramics.²⁹ However, in Ti-rich BaTiO₃ samples, the sodium impurities react with the excess of TiO₂ with formation of discrete Na₄TiO₄ particles.³⁰ In the light of the previous considerations a profound influence of the Ba/Ti ratio on the grain boundary structure and the thickness of the grain boundary layer is not unlikely. Therefore, is not surprising that the relative dielectric constant of the present samples

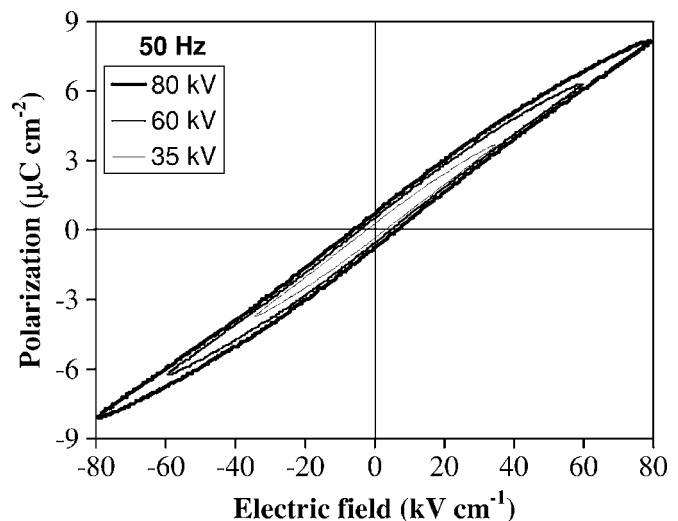


FIG. 5. Polarization-electric field loops of a dense nanocrystalline BaTiO₃ ceramic with grain size of ≈ 30 nm collected at 50 Hz and at different values of the field amplitude 35, 60, and 80 kV cm⁻¹.

with grain size of 30 nm is about twice that of the ceramics with grain size of 50 nm reported in the previous study.¹⁴

Macroscopic polarization hysteresis. Figure 5 shows the as-measured, noncompensated macroscopic $P(E)$ loops under a sinusoidal wave of 50 Hz for three different values (35, 60, and 80 kV cm⁻¹) of the field amplitude. The system exhibits very small hysteresis with almost linear dependence of $P(E)$ below 40 kV cm⁻¹. A small deviation from linearity is observed at higher field amplitudes. For the highest value of the field amplitude the remnant polarization (P_r) is ≈ 0.7 $\mu\text{C}/\text{cm}^2$ and the coercive field (E_c) is ≈ 5 kV cm⁻¹. [Note: for the $P(E)$ loops reported in Fig. 5 is not completely appropriate to speak of remnant polarization and coercive field because there is no evidence of macroscopic switching. In this case, P_r and E_c simply denote the polarization at zero field and the field at zero polarization.] For comparison, in good quality coarse (grain size > 10 μm) ceramics $P_r \approx 10$ $\mu\text{C}/\text{cm}^2$ and $E_c \approx 3$ –5 kV cm⁻¹, with good saturation of polarization above 10 kV cm⁻¹. A progressive lowering of remnant polarization and hysteresis with decreasing grain size, as well as the gradual tilting of the $P(E)$ loop, was reported by Frey *et al.*¹⁵ and by Takeuchi *et al.*²⁶ For bulk dense ceramics with grain size of the order of 100–200 nm, P_r was ≈ 2 $\mu\text{C}/\text{cm}^2$ and $E_c \approx 1$ kV cm⁻¹ (field amplitude up to 25 kV cm⁻¹). The Landau-Ginzburg-Devonshire theory predicts that the square of the spontaneous polarization is proportional to the tetragonal lattice strain.³¹ However, this intrinsic effect alone can not explain the observed behavior. Given the value of $c/a-1$ of the present nanocrystalline BaTiO₃, the spontaneous polarization in nanocrystalline ceramics is predicted to be still rather large, half of the value reported for coarse ceramics. Therefore it should be admitted that the macroscopic ferroelectric properties of nanocrystalline BT ceramics are dominated by extrinsic effects, while intrinsic effects have only a marginal influence.

A remarkable increase of P_r with increasing annealing temperature has been observed for polycrystalline thin films

of BaTiO₃,³² SrBi₂Ta₂O₉,³³ and PbTiO₃.³⁴ This behavior can be correlated to the growth of the grain size with the annealing temperature. At low annealing temperature, when the grains have a size comparable to that of the single domain, the domain structure becomes very stable under an external field, meaning that domain wall movement and nucleation of new domains becomes difficult.³⁴ The absence of 90° domains can strongly affect the polarization behavior and the piezoelectric properties of ferroelectric ceramics. It is known that for grain sizes below 300–500 nm there is a reduced number of 90° domains^{4,14,15} in BaTiO₃. According to Damjanovic,³⁵ a strong reduction of the remnant polarization and of the Rayleigh constant in ceramics is expected if 90° domains are absent or pinned by defects. The measurement of the direct piezoelectric effect in coarse and submicron (grain size: 0.7 μm) BaTiO₃ ceramics has shown a contribution of 90° domain walls in both materials.³⁶ However, the activity of the domain walls in the fine grain ceramics was weaker than in the coarse samples. It was concluded that the domain walls in fine grain ceramics are clamped to a considerable degree. In any case, the fine grain samples displayed well-defined piezoelectric effect and could be poled under a field of 20 kV cm⁻¹, in agreement with the well-saturated hysteresis loops still observed in ceramics with submicron grain size.^{15,26} Therefore, even if the domains are already considerably clamped in submicron materials, the suppression of macroscopic switching is a feature of ceramics with grain size well below 100 nm.

A further effect which can contribute to the depression of the ferroelectric properties has to be considered when there is a high density of grain boundaries, as in nanocrystalline ceramics. Because of the existence of a low-permittivity, non-ferroelectric grain boundary layer, the polarization decays at the surface of the ferroelectric grains and this variation creates a depolarization field. According to theoretical considerations³⁷ as well as modelling of polarization switching with grain boundary effect,³⁸ this depolarization field causes a decrease of the effective polarization with respect to the bulk value. Therefore, poor ferroelectric properties are expected in polycrystalline ceramics with very small grain size (<50 nm), as those investigated in the present study. On the basis of the above considerations, it is proposed that the combined effect of (i) a simple domain structure which cannot readily deform under an external field, (ii) the pinning of the domain walls and the suppression of large-scale domain switching induced by the grain boundaries and/or the defects segregated at grain boundaries, and (iii) the depolarizing field arising from the presence of a low-permittivity nonferroelectric grain boundary layer, results in a strong depression of the ferroelectric character and, consequently, in the observed slim and nearly linear $P(E)$ loops.

In order to check if the recorded $P(E)$ loops really correspond to those expected for a ferroelectric with strongly pinned domains and to find their characteristics, a quantitative Rayleigh analysis was performed. The phenomenological law of Rayleigh originally proposed for magnetic materials³⁹ and later extended to other hysteretic processes^{40–42} describes the irreversible movement of domain walls under an ac field in a medium with randomly distributed defects acting as pinning centers. In the Rayleigh

region, the $P(E)$ loop can be expressed by two parabolic functions⁴²

$$P(E) = (\varepsilon_{\text{in}} + 2\alpha E_0)E \pm \alpha(E_0^2 - E^2), \quad (2)$$

in which ε_{in} is the zero-field (or initial) permittivity, α the Rayleigh coefficient, E_0 the field amplitude, and E the actual value of the electric field. The + stands for decreasing field and the - for increasing field. A polynomial regression of the $P(E)$ data at each field amplitude by Eq. (2) has allowed to obtain the field amplitude-dependence of the permittivity $\varepsilon_r(E_0)$ and to calculate the value of the Rayleigh constant for the present nanocrystalline BaTiO₃ ceramics. The expression of the permittivity in the Rayleigh region is

$$\varepsilon_r(E_0) = \varepsilon_{\text{in}} + 2\alpha E_0. \quad (3)$$

Three regimes of dielectric behavior, defined by the threshold fields $E_{t,1}$ and $E_{t,2}$, were identified in the $\varepsilon_r - E_0$ plot, as usually observed in polycrystalline ferroelectrics.⁴² In the low field region, $E_0 < E_{t,1}$, ε_r was nearly independent of the field amplitude. In this region, permittivity is due to intrinsic lattice contribution and reversible domain wall vibrations.⁴² Large scale domain wall mobility is inhibited by the pinning effect of charged defects. An increase of the zero-field permittivity from $\varepsilon_{\text{in}} = 1304$ at 100 Hz to 1365 at 1 Hz was found, in agreement with the trend observed in the permittivity data of Fig. 2. The value of $E_{t,1}$ was 5–10 kV cm⁻¹, and can be compared with threshold fields of less than 0.1 kV cm⁻¹ in coarse BaTiO₃ ceramics and ≈ 3 kV cm⁻¹ in commercial acceptor-doped hard PZT ceramic.^{42,43} In the intermediate (Rayleigh) region ($E_{t,1} < E_0 < E_{t,2}$), a linear dependence of ε_r on the field amplitude is observed, according to Eq. (3). The values of α obtained from the fit 1–2 $\times 10^{-16}$ F/V, are much smaller than the value of 6.5×10^{-14} F/V reported for a pure coarse BaTiO₃ ceramic.⁴² Values closer to the present results were reported for hard PZT ceramics [5.9×10^{-15} F/V (Ref. 42)] and PZT thin films [6.9×10^{-16} F/V (Ref. 40)]. Deviation from the linear behavior started at fields larger than $E_{t,2} = 25$ –30 kV cm⁻¹. Values of $E_{t,2}$ reported in the literature are ≈ 0.8 kV cm⁻¹ for pure BaTiO₃ ceramics, ≈ 5 kV cm⁻¹ for acceptor-doped BaTiO₃ ceramics, 17 kV cm⁻¹ for a commercial acceptor-doped hard PZT ceramic⁴² and ≈ 50 kV cm⁻¹ for thin film PZT.⁴⁰ According to the conventional interpretation, $E_{t,2}$ represents the critical field required to initiate partial domain switching.⁴² However, in the present case, it is not clear if the deviation from the Rayleigh behavior is related to the incipient switching process or to other nonlinearities and dissipation processes possibly activated at such high values of the applied field.

The previous analysis gives evidence that the polarization hysteresis of nanocrystalline BT ceramics up to a field amplitude of 25–30 kV cm⁻¹ is typical of the subswitching field region in ferroelectric ceramics. According to the statistic theory of Boser,⁴⁴ an inverse proportionality between the coefficient α and the concentration of defects in ferroelectric materials exists. Therefore, the low value of the Rayleigh constant and the expected large value of the coercive field (>80 kV cm⁻¹) indicate that the irreversible domain wall

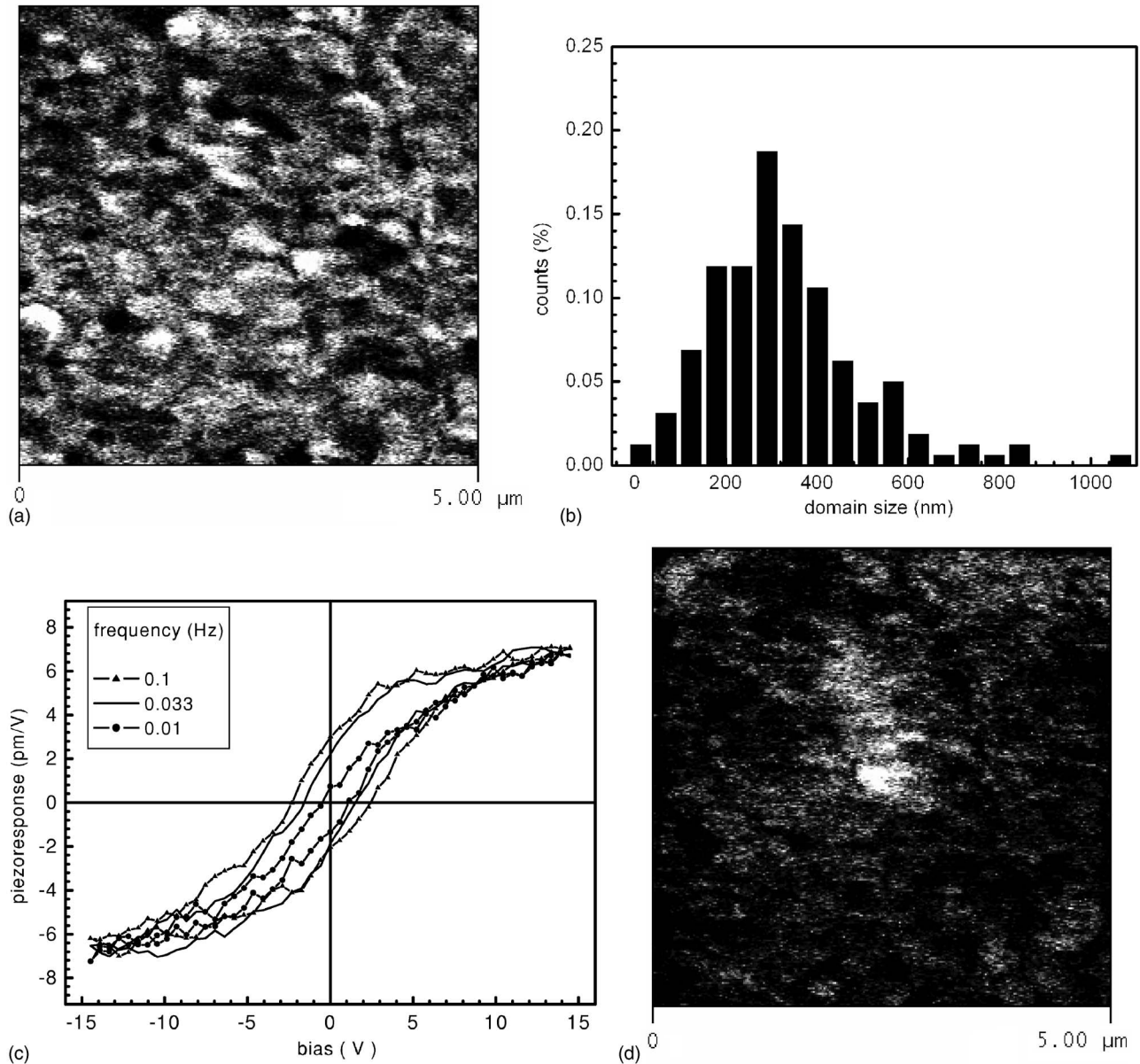


FIG. 6. Piezoresponse measurements of dense nanocrystalline BT ceramic with grain size of ≈ 30 nm. (a) Piezoresponse image (scan area $5 \times 5 \mu\text{m}^2$). (b) Frequency distribution of domain sizes. (c) Piezoelectric hysteresis loops recorded at different frequencies. (d) Piezoresponse image (scan area $5 \times 5 \mu\text{m}^2$) after the application of a 40 V poling voltage.

displacement and switching in nanocrystalline BaTiO_3 is strongly inhibited by defects.³⁵ It is proposed that the defects responsible for the pinning of the domains and the hindrance of large-scale switching are strictly related to the grain boundaries. As shown in the next section, piezoresponse force microscopy has revealed transgranular domains with average lateral size of ≈ 250 nm. Consequently, each domain comprises many grains, and the charged defects at the grain boundary can exert a strong influence on domain wall mobility and switching, leading to a frozen polarization.

It is also worth noting that the low permittivity, nonferroelectric grain boundaries lead to a reduction of the effective field acting on the ferroelectric cores in comparison to the applied field. Using a brick-wall model for the ceramic, taking $\epsilon_d \approx 100$ as proposed in the foregoing discussion on the

Curie-Weiss analysis and assuming a permittivity of ≈ 3000 for the ferroelectric cores (a reasonable value, according to Ref. 15), the effective field in the ferroelectric region was calculated to be only $\approx 50\%$ of the applied field. This means that the values of the maximum field amplitude and the threshold fields $E_{t,1}$ and $E_{t,2}$ should be divided by a factor of 2.

Local piezoresponse measurements. The high sensitivity of piezoresponse force measurements even at nanoscale, makes this method suitable to study the local switching properties in nanostructured ferroelectrics.^{10,45–47} A typical piezoresponse image corresponding to the out-of-plane component of polarization is shown in Fig. 6(a). Owing to the relatively large radius of the tip, estimated to be of the order of 50 nm, the lateral resolution is limited and finer details of the do-

main structure, if any, cannot be observed. The image shows a relatively strong black/white contrast, an indication of the presence of a ferroelectric domain structure in the as-prepared ceramic samples. The lateral size of the domains is apparently between 50 and 500 nm and the average size is of the order of 250 nm [Fig. 6(b)]. Therefore a single domain comprises of a considerable number of grains. Because the resolution is limited by the tip radius, we cannot exclude the presence of smaller domains, having the size of the grains or even smaller in those areas which appear gray in the image. Repeated scanning of the surface with an ac voltage on the tip often results in the destruction of the original domain structure, suggesting that the applied testing voltage of 0.25 V amplitude is large enough to switch the domains in the near vicinity of the surface. This is the consequence of the very high permittivity of the sample and of the particular geometry of the tip-sample system,⁴⁸ making the field highly nonuniform near the tip apex. Indeed, an estimation of the electric field distribution in the sample using a simple electrostatic model⁴⁷ shows that, for our experiment, the electric field below the tip drops by four orders of magnitude over the first 50 nm layer of the sample below the surface.

Local hysteresis measurements were performed by keeping the AFM tip fixed above the surface and applying a large, low frequency (0.01 to 0.1 Hz) bias superimposed over the small ac excitation while recording the piezoresponse signal in various locations. Figure 6(c) shows a typical hysteresis loop collected at different frequencies. The coercivity increases with increasing frequency while the saturation piezoresponse is practically unchanged. This is an indication that the observed loops are not induced by charge accumulation under the AFM tip (which should have an additive effect and therefore leading to a stronger signal at maximum voltage for longer cycling periods) but more likely, related to the local ferroelectric behavior of the sample. As the dc bias is applied for longer periods of time, the induced polarization relaxes under the influence of both the ac testing voltage and of the depolarizing field produced by the surrounding medium with a high concentration of grain boundaries. As suggested by the time scale of the hysteresis loops, this relaxation time is of the order of few 100 s. Indeed, application of high voltage (40 V) poling pulses to the sample surface resulted in the formation of domains with a lateral size in the 1 μm range [Fig. 6(d)], which disappeared within 5–10 min after the removal of the voltage. In a previous piezoresponse microscopy investigation⁴⁵ performed on BT ceramics with a grain size of 50 nm the induced domain structure was stable for rather long times (at least 8 h). This means that the grain size (30 nm) of the present samples is close to a critical value required for the stability of the field-induced domain structure.

The apparent contradiction between the quasilinear $P(E)$ macroscopic loops (Fig. 5), and the evident local switching (Fig. 6) and nonlinear character at local scale can be understood by considering the particularities of the experimental setup of the AFM-piezoresponse system by comparison with the plane-parallel configuration of the macroscopic switching experiment. The switching mechanism in the two cases might be very different from the first moments of nucleation-growth process, since the highly inhomogeneous field in the

AFM experiment causes itself a nucleation in the region under the tip, whereas in the macroscopic experiments nucleation starts at defective zones as grain boundaries and the ceramic/electrode interface.⁴⁸ Moreover, the very high fields acting in the small region under the tip apex, which causes the complete local switching at nanoscale, are inaccessible experimentally in the macroscopic switching experiments. Finally, it should be considered that the mechanical boundary conditions of grains on the surface are rather different from those in the interior of the ceramic. Very likely, local switching occurs even in the macroscopic experiments at locations where nucleation of domains with opposite polarization orientation is energetically favorable.

The overall results of this investigation suggest a somewhat different behavior of nanocrystalline ceramics in comparison to that anticipated by the thermodynamic theory for isolated ferroelectric particles⁵ when the grain size is reduced to the nanometric scale. The theory predicts a progressive decrease of the Curie temperature, of the spontaneous lattice strain and of the intrinsic polarization with decreasing particle size until a critical size corresponding to the transition to the cubic paraelectric phase and disappearance of ferroelectricity is reached.⁵ In contrast, for nanoceramics, the downscaling of properties with grain size is masked by the extrinsic effects exerted by the grain boundaries, such as the pinning of the domain walls and the blocking of the polarization. Therefore, even though the material retains a polar crystal structure, it will exhibit very poor ferroelectric properties. In the limit case, the ferroelectric behavior will be absent and a polar phase with nonswitchable polarization (as in a pyroelectric system) will be obtained. The BaTiO₃ ceramics with grain size of 30 nm investigated in the present study are deemed to be close to this kind of “phase transition.”

A further consequence of the frozen domain structure is that the superparaelectric behavior cannot be induced in ferroelectric ceramics by simply reducing the grain size. Up to now there is not yet a convincing evidence of size induced superparaelectric behavior in ferroelectrics, although this was postulated by analogy with magnetic systems.^{7,8} The superparaelectric behavior implies that the system can easily flip, at local level, between states with different polarization orientation separated by small energy barriers comparable with the thermal energy. In contrast, for the present nanoceramics, the energy barrier is extremely high. It turns out that, at least in dense ceramics, the superparaelectric state can be hardly realized by decreasing the grain size.

IV. SUMMARY AND CONCLUSIONS

The dielectric properties as well as the macroscopic and local ferroelectric properties of dense (97% relative density) nanocrystalline BaTiO₃ ceramics with grain size of ≈ 30 nm prepared by spark plasma sintering were investigated. There are no previous reports on the properties of bulk dense ceramics with such a small grain size. The main results and conclusions of the present work can be summarized as follows.

(1) The high dielectric constant (about 1500–1600), the low losses ($\approx 2\%$ in 10^{-1} to 10^5 Hz) and the high electrical

dc resistivity ($\approx 10^{13} \Omega \text{ cm}$) at room temperature make nanocrystalline BaTiO_3 a potential candidate for the realization of multilayer ceramic capacitors with very thin ($< 1 \mu\text{m}$) layers. The field-independent permittivity up to an ac field amplitude of $\approx 10 \text{ kV cm}^{-1}$, the small ferroelectric hysteresis and the expected high breakdown field are significant advantages for dielectric applications. The measured permittivity and the observed shift of the Curie-Weiss temperature are compatible with the existence of a non ferroelectric grain boundary layer with a thickness of $\approx 1 \text{ nm}$.

(2) The measurement of the dielectric properties as a function of temperature (which show a maximum in the permittivity, and a Curie-Weiss behavior at temperatures above the maximum) and the noncubic (polar) crystal structure revealed by XRD indicate a ferroelectric behavior. On the contrary, the polarization hysteresis show very slim and nearly linear loops without evidence of macroscopic switching up to the maximum field amplitude used in this study (80 kV cm^{-1}). It is proposed that the suppression of ferroelectric hysteresis in nanocrystalline BaTiO_3 ceramics results from a frozen domain structure which is stable under an external field, meaning that domain walls movement and nucleation of new domains becomes difficult when the grain size attains values of few tens of nanometers. Rayleigh analysis of the measured $P(E)$ loops supports this interpretation. The threshold field corresponding to the onset of the irreversible domain wall movement as well as the Rayleigh constant takes value which are typical of doped ferroelectric ceramics with strongly pinned domain walls rather than of pure coarse barium titanate. Grain boundaries and charged defects segregated at grain boundaries are considered to be responsible for the clamping of the domain walls and the hindrance of polarization reversal. The absence or a low density of 90° domains in nanocrystalline BaTiO_3 ceramics can significantly contribute to the depression of the ferroelectric properties. In addition, the effective polarization in nanocrystalline ceramics is expected to be reduced by the depolarization field associated to the lowpermittivity nonferroelectric grain boundary layer.

(3) Out-of-plane piezoresponse hysteresis loops recorded by piezoresponse force microscopy provide evidence of polarization switching and ferroelectric behavior at local scale. Piezoresponse images show as-grown domains extending

over a considerable number of grains. Application of local poling voltage pulses induces formation of domain structures which disappear in a time of minutes after removal of the voltage. These results indicate that even in the macroscopic experiments only local switching at some locations of easier nucleation of domains with opposite orientation of polarization is probably realized. In any case, comparison with the macroscopic polarization experiments is not straightforward because the boundary conditions, the distribution and amplitude of the applied field as well as the switching mechanisms are radically different.

(4) The overall results indicate that the dielectric and ferroelectric behavior of dense nanocrystalline BaTiO_3 ceramics is dominated by extrinsic effects exerted by the grain boundaries. These extrinsic effects mask the progressive downscaling of ferroelectric properties with grain size expected from the theory of small ferroelectric particles. When the grain size is small enough, transition to a polar phase with non-switchable polarization (as in a pyroelectric system) is expected. In other words, suppression of ferroelectricity in ceramics is not related to the size-induced stabilization of the cubic paraelectric phase as predicted by theory but, rather, to the existence of a completely frozen domain structure. It is deemed that the present nanocrystalline ceramics with grain size of 30 nm are very close to this limit.

(5) The existence of a frozen domain structure implies that the superparaelectric behavior cannot be induced in ferroelectric ceramics by simply reducing the grain size. The superparaelectric behavior implies that the system can easily flip, at local level, between states with different polarization orientation separated by small energy barriers comparable with the thermal energy. In contrast, for the present nanoceramics, the energy barrier is extremely high, as proved by the impossibility of switching the macroscopic polarization even at very high fields.

ACKNOWLEDGMENTS

This work was supported in part by the Italian Ministry of Education, University and Research through a PRIN project. C.H. acknowledges financial support from NanoQuebec Project No. 109 and L.M. from CNCSIS A624 Romania grant.

*Electronic address: v.buscaglia@ge.ieni.cnr.it

†Electronic address: zhao@inorg.su.se

¹A. Rae, M. Chu, and V. Ganine, in *Dielectric Ceramic Materials*, Vol. 100 of *Ceramic Transactions*, edited by K. M. Nair and A. S. Bhalla (The American Ceramic Society, Westerville, OH, 1999), pp. 1–12.

²T. G. Reynolds III, *Am. Ceram. Soc. Bull.* **80**, 29 (2001); C. A. Randall, *J. Ceram. Soc. Jpn.* **109**, S2 (2001).

³K. Kinoshita and A. Yamaji, *J. Appl. Phys.* **47**, 371 (1976).

⁴G. Arlt, D. Hennings, and G. de With, *J. Appl. Phys.* **58**, 1619 (1985).

⁵W. L. Zhong, Y. G. Wang, P. L. Zhang, and B. D. Qu, *Phys. Rev.*

B **50**, 698 (1994); S. Li, J. A. Eastman, Z. Li, C. M. Foster, R. E. Newnham, and L. E. Cross, *Phys. Lett. A* **212**, 341 (1996); B. Jiang and L. A. Bursill, *Phys. Rev. B* **60**, 9978 (1999).

⁶A. M. Bratkovsky and A. P. Levanyuk, *Phys. Rev. Lett.* **94**, 107601 (2005).

⁷T. M. Shaw, S. Trolier-McKinstry, and P. C. McIntyre, *Annu. Rev. Mater. Sci.* **30**, 263 (2000); J. F. Scott, F. D. Morrison, M. Miyake, P. Zubko, X. Lou, V. M. Kugler, S. Rios, M. Zhang, T. Tatsuta, O. Tsuji, and T. J. Leedham, *J. Am. Ceram. Soc.* **88**, 1691 (2005); A. Rüdiger, T. Schneller, A. Roelofs, S. Tiedke, T. Schmitz, and R. Waser, *Appl. Phys. A* **80**, 1247 (2005).

⁸K. Ishikawa, K. Yoshikawa, and N. Okada, *Phys. Rev. B* **37**,

- 5852 (1988); K. Uchino, E. Sadanaga, and T. Hirose, *J. Am. Ceram. Soc.* **72**, 1555 (1989); W. L. Zhong, B. Jiang, P. L. Zhang, J. M. Ma, H. M. Cheng, Z. H. Yang, and L. X. Li, *J. Phys.: Condens. Matter* **5**, 2619 (1993); D. McCauley, R. E. Newnham, and C. A. Randall, *J. Am. Ceram. Soc.* **81**, 979 (1998); K. Ishikawa and T. Uemori, *Phys. Rev. B* **60**, 11841 (1999); S. Tsunekawa, S. Ito, T. Mori, K. Ishikawa, Z.-Q. Li, and Y. Kawazoe, *ibid.* **62**, 3065 (2000); R. Böttcher, C. Klimm, D. Michel, H.-C. Semmelhack, G. Völkel, H.-J. Gläsel, and E. Hartmann, *ibid.* **62**, 2085 (2000); A. Roelofs, T. Schneller, K. Szot, and R. Waser, *Appl. Phys. Lett.* **81**, 5231 (2002); M. Yashima, T. Hoshina, D. Ishimura, S. Kobayashi, W. Nakamura, T. Tsurumi, and S. Wada, *J. Appl. Phys.* **98**, 014313 (2005).
- ⁹J. Zhang, Z. Yin, M.-S. Zhang, and J. F. Scott, *Solid State Commun.* **118**, 241 (2001); M. Dawber, P. Chandra, P. B. Littlewood, and J. F. Scott, *J. Phys.: Condens. Matter* **15**, L393 (2003).
- ¹⁰M.-W. Chu, I. Szafraniak, R. Scholz, C. Harnagea, D. Hesse, M. Alexe, and U. Gösele, *Nat. Mater.* **3**, 87 (2004).
- ¹¹C. H. Ahn, K. M. Rabe, and J.-M. Triscone, *Science* **303**, 488 (2004); D. D. Fong, G. B. Stephenson, S. K. Streiffer, J. A. Eastman, O. Auciello, P. H. Fuoss, and C. Thompson, *ibid.* **304**, 1650 (2004); J. Junquera and Ph. Ghosez, *Nature (London)* **422**, 506 (2003).
- ¹²M. M. Saad, P. Baxter, R. M. Bowman, J. M. Gregg, F. D. Morrison, and J. F. Scott, *J. Phys.: Condens. Matter* **16**, L451 (2004).
- ¹³W. R. Buessem, L. E. Cross, and A. K. Goswami, *J. Am. Ceram. Soc.* **49**, 33 (1966); **49**, 36 (1966).
- ¹⁴Z. Zhao, V. Buscaglia, M. Viviani, M. T. Buscaglia, L. Mitoseriu, A. Testino, M. Nygren, M. Johnsson, and P. Nanni, *Phys. Rev. B* **70**, 024107 (2004).
- ¹⁵M. H. Frey, Z. Xu, P. Han, and D. A. Payne, *Ferroelectrics* **206-207**, 337 (1998).
- ¹⁶A. Yu. Emelyanov, N. A. Pertsev, S. Hoffmann-Eifert, U. Böttger, and R. Waser, *J. Electroceram.* **9**, 5 (2002).
- ¹⁷A. V. Polotai, A. V. Ragulya, and C. A. Randall, *Ferroelectrics* **288**, 93 (2003).
- ¹⁸I. Rychetský, J. Petzelt, and T. Ostapchuk, *Appl. Phys. Lett.* **81**, 4224 (2002).
- ¹⁹X. Guo, C. Pithan, C. Ohly, C.-L. Jia, J. Dornseiffer, F.-H. Hae-gel, and R. Waser, *Appl. Phys. Lett.* **86**, 082110 (2005).
- ²⁰A. Testino, M. T. Buscaglia, M. Viviani, V. Buscaglia, and P. Nanni, *J. Am. Ceram. Soc.* **87**, 79 (2004); A. Testino, M. T. Buscaglia, V. Buscaglia, M. Viviani, C. Bottino, and P. Nanni, *Chem. Mater.* **16**, 1536 (2004).
- ²¹F. Valdivieso, M. Pijolat, C. Magnier, and M. Soustelle, *Solid State Ionics* **83**, 283 (1996); P. R. Rios, T. Yamamoto, T. Kondo, and T. Sakuma, *Acta Mater.* **46**, 1617 (1998); Y. K. Cho, S.-J. Kang, and D. Y. Yoon, *J. Am. Ceram. Soc.* **87**, 119 (2004).
- ²²M. E. Lines and A. M. Glass, *Principles and Applications of Ferroelectrics and Related Materials* (Oxford University Press, Oxford, 1977).
- ²³D. E. Rase and R. Roy, *J. Am. Ceram. Soc.* **38**, 102 (1955).
- ²⁴J. H. Hwang and Y. H. Han, *Electrochemistry (Tokyo, Jpn.)* **68**, 423 (2000).
- ²⁵S. K. Streiffer, C. Basceri, C. B. Parker, S. E. Lash, and A. I. Kingon, *J. Appl. Phys.* **86**, 4565 (1999).
- ²⁶T. Takeuchi, C. Capiglia, N. Balakrishnan, Y. Takeda, and H. Kageyama, *J. Mater. Res.* **17**, 575 (2002).
- ²⁷S. B. Lee, W. Sigle, and M. Rühle, *Acta Mater.* **50**, 2151 (2002).
- ²⁸B.-K. Lee, S.-Y. Chung, and S.-J. Kang, *Acta Mater.* **48**, 1575 (2000); S.-Y. Choi and S.-J. Kang, *ibid.* **52**, 2937 (2004).
- ²⁹Y.-M. Chiang and T. Takagi, *J. Am. Ceram. Soc.* **73**, 3278 (1990).
- ³⁰M.-H. Lin, J.-F. Chou, and H.-Y. Lu, *J. Am. Ceram. Soc.* **83**, 2155 (2000).
- ³¹A. F. Devonshire, *Philos. Mag.* **40**, 1040 (1949).
- ³²Y. Yamashita, H. Yamamoto, and Y. Sakabe, *Jpn. J. Appl. Phys., Part 1* **43**, 6521 (2004).
- ³³A. Li, D. Wu, H. Ling, T. Yu, M. Wang, X. Yin, Z. Liu, and N. Ming, *J. Appl. Phys.* **88**, 1035 (2000); H.-Y. Chou, T.-M. Chen, and T.-Y. Tseng, *Mater. Chem. Phys.* **82**, 826 (2003).
- ³⁴S. B. Ren, C. J. Lu, J. S. Liu, H. M. Shen, and Y. N. Wang, *Phys. Rev. B* **54**, R14337 (1996); S. B. Ren, C. J. Lu, H. M. Shen, and Y. N. Wang, *ibid.* **55**, 3485 (1997).
- ³⁵D. Damjanovic, *Rep. Prog. Phys.* **61**, 1267 (1998).
- ³⁶M. Demartin and D. Damjanovic, *Appl. Phys. Lett.* **68**, 3046 (1996).
- ³⁷R. Kretschmer and K. Binder, *Phys. Rev. B* **20**, 1065 (1979); A. K. Tagantsev, V. O. Sherman, K. F. Astafiev, J. Venkatesh, and N. Setter, *J. Electroceram.* **11**, 5 (2003).
- ³⁸S.-J. Kim, *J. Appl. Phys.* **92**, 2668 (2002).
- ³⁹L. Rayleigh, *Philos. Mag.* **23**, 225 (1887).
- ⁴⁰D. V. Taylor and D. Damjanovic, *J. Appl. Phys.* **82**, 1973 (1997).
- ⁴¹D. Damjanovic and M. Demartin, *J. Phys. D* **29**, 2057 (1996).
- ⁴²D. A. Hall, *Ferroelectrics* **223**, 319 (1999); D. A. Hall and P. J. Stevenson, *ibid.* **228**, 139 (1999); D. A. Hall, *J. Mater. Sci.* **36**, 4575 (2001).
- ⁴³K. Wu and W. A. Schulze, *J. Am. Ceram. Soc.* **75**, 3385 (1992).
- ⁴⁴O. Boser, *J. Appl. Phys.* **62**, 1344 (1987).
- ⁴⁵L. Mitoseriu, C. Harnagea, P. Nanni, A. Testino, M. T. Buscaglia, V. Buscaglia, M. Viviani, Z. Zhao, and M. Nygren, *Appl. Phys. Lett.* **84**, 2418 (2004).
- ⁴⁶V. V. Shvartsman, A. L. Kholkin, A. Orlova, D. Kiselev, A. A. Bogomolov, and A. Sternberg, *Appl. Phys. Lett.* **86**, 202937 (2005).
- ⁴⁷C. Harnagea and A. Pignolet, in *Nanoscale Characterization of Ferroelectric Materials*, edited by A. Gruverman and M. Alexe (Springer, Berlin, 2004), pp. 45–85.
- ⁴⁸V. V. Shvartsman, N. A. Pertsev, J. M. Herrero, C. Zaldo, and A. L. Kholkin, *J. Appl. Phys.* **97**, 104105 (2005).